Supporting Information

for

Photo-controlled Targeted Intracellular Delivery of Both Nitric Oxide and Singlet Oxygen Using Fluorescence-trackable Ruthenium Nitrosyl Functional Nanoplatform

Hui-Jing Xiang,[†] Lu An,[‡] Wei-Wei Tang, [†] Shi-Ping Yang,[‡*] and Jin-Gang Liu[†*]

[†]*Key Laboratory for Advanced Materials of MOE & Department of Chemistry, East China University of Science and Technology, Shanghai, 200237, P. R. China, E-mail: liujingang@ecust.edu.cn*

[‡]*Key Laboratory of Resource Chemistry of MOE & Shanghai Key Laboratory of Rare Earth Functional Materials, Shanghai Normal University, Shanghai, 200234, P. R. China,* E-mail: *shipingy@shnu.edu.cn*

1. Chemicals:

All reagents were purchased commercially and used without further purification unless otherwise noted. Acetonitrile (CH_3CN) for cyclic voltammetry and spectroscopic measurements was purified by firstly distilling from P_2O_5 and redistilled from CaH_2. The compounds DAMBO[S1], (8-(3,4-diaminophenyl)-4,4-difluoro-1,3,5,7-tetramethyl-4-bora3a,4a-diaza-s-indacene), (4-NH_2)-C_6H_4-PO_3H((4-aminobenzyl)phosphonic acid)[S2], [Ru(tpy^{COOH})Cl_3] (tpy^{COOH} = (2,2':6',2''-terpyridine)-4'-carboxylic acid)[S3,S4] and CHDDE (sodium 1,3-cyclohexadiene-1,4-diethanoate)[S5] were prepared according to literatures.

2. General Techniques:

^1H NMR spectra were recorded on Bruker AV400 spectrometer (400 MHz). ESI mass spectra were performed on Micromass LCTTM mass spectrometer. Transmission electron microscopy (TEM) was performed on a JEOL JEM-2011 transmission electron microscope operating at 100 kV. Powder X-ray diffraction (XRD) analysis was performed on Bruker D8 ADVANCE X-Ray Diffractomer. The ruthenium content on TiO_2 nanoparticles was measured on a Falcon Energy dispersive spectrometer. FTIR spectra were recorded on a Shimadzu Fourier transform infrared spectrometer (IRPrestige-21). UV-vis absorption spectra were recorded on a Shimadzu UV-visible spectrophotometer (UV-2600). Fluorescence studies were carried out on a Horiba Fluoromax-4 fluorescence spectrophotometer. Cyclic voltammetry (CV) were performed on a CH Instrument Model 760D potentiostat in a standard three-electrode cell, a glassy carbon electrode covered by a thin film of **1** as working electrode, a platinum wire as the counter electrode, and a Ag/AgCl electrode as the reference electrode. Cyclic voltammograms were recorded at room temperature in CH_3CN with 0.1 M *n*-Bu_4NBF_4 as the electrolyte.

Light source: Asahi Spectra Max 303 Xe lamp equipped with a 300–600 nm ultraviolet visible module, 1.0 collimator lens and a longpass filter UV400. The intensity of visible light irradiation (λ > 400nm) on the sample cell was measured by using a CEL-NP 2000 intensity meter. The amount of NO released was measured using a NO-sensitive electrode (World Precision Instrument, ISO-NO meter, equipped with a TBR1025 free radical analyzer for measuring nitric oxide from 0.3 nM to 100 μM.). The tip of the electrode was placed outside the light path. The electrode was accurately calibrated by mixing standard solutions of $NaNO_2$ with

H_2SO_4 (0.1 M) and KI (0.1 M), according to the protocol indicated in the manufacturer manual. The amperometric data collected from the electrode was then converted into the corresponding nitric oxide concentration. Fluorescence images were acquired by using a Leica TCS SP5 II inverted microscope with a Leica DMI 6000B confocal scanning system. Flow cytometry (FCM) was performed on a Beckman Coulter flow cytometer (Quanta SC, USA).

3. Methods.

The {Ru-NO@TiO_2 NPs} nanoplatform was prepared according to Scheme S1.

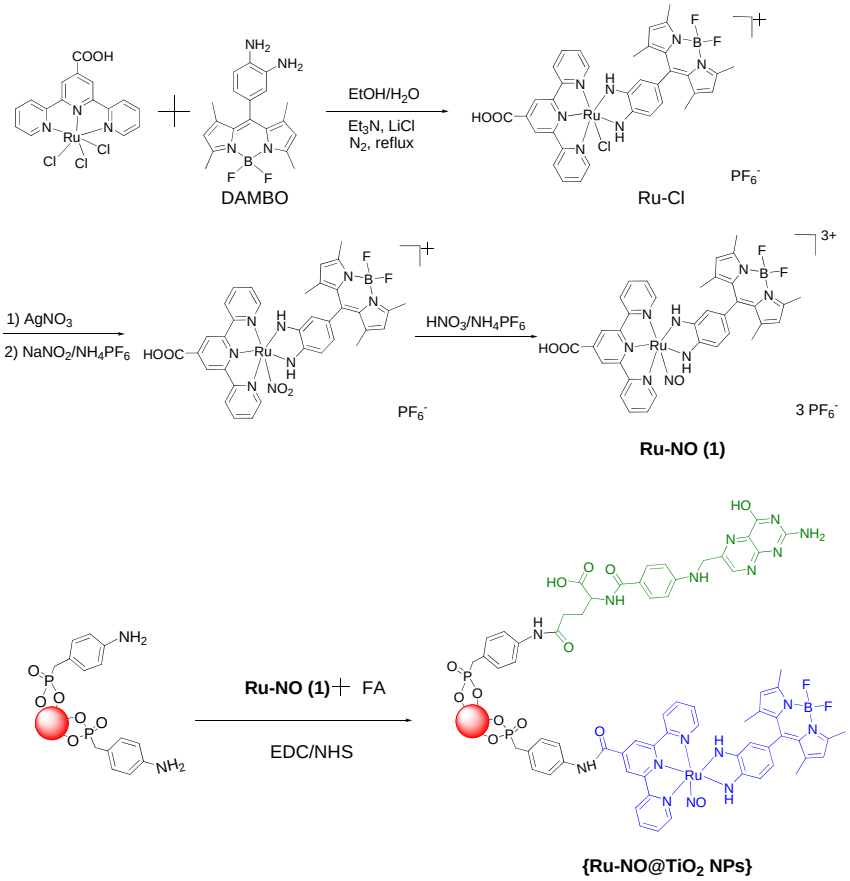

Scheme S1 Preparation route for the {Ru-NO@TiO_2 NPs} nanoplatform.

Synthesis of [(tpy^{COOH})Ru(DAMBO)(Cl)](PF_6)

To a mixture of EtOH-H_2O (40 mL, 3:1, v/v) containing LiCl (85 mg, 2.0 mmol) and Et_3N (0.4 mL), Ru(tpy^{COOH})Cl_3 (150 mg, 0.31 mmol) and DAMBO (8-(3,4-diaminophenyl)-4,4-difluoro-1,3,5,7-tetramethyl-4-bora3a,4a-diaza-s-indacene) (117 mg, 0.33 mmol) were added. Then the resulting mixture was heated at reflux for 8 h under N_2 atmosphere. While hot the suspension was filtered through a pad of Celite. The resulting clear deep red solution was

concentrated to a few milliliters and excess saturated aqueous solution of NH_4PF_6 was added. Then the mixture was stored at 5 °C overnight. The red brown solid precipitate was filtered, washed with water and Et_2O (15 mL), dried in vacuo. Yield: 182.3 mg (64.3%). **^{1}H NMR** (400 MHz, CD_3OD) δ 9.06 (s, 2H), 8.64-8.50 (m, 2H), 8.00 (d, 2H), 7.53-7.38 (m, 5H), 7.20-7.01 (m, 2H), 6.06 (s, 2H), 2.45 (s, 6H), 1.55 (s, 6H) ppm. **ESI-MS** *m/z* $[M\text{-}PF_6]^+$: calcd. 766.1, found 766.2.

Synthesis of [(tpy^{COOH})Ru(DAMBO)(NO_2)](PF_6).

[(tpy^{COOH})Ru(DAMBO)(Cl)](PF_6) (100 mg, 0.11 mmol) and an excess of $AgNO_3$ (37 mg, 0.22 mmol) were taken in 30 mL of CH_3CN-H_2O (1:1, v/v) and heated at reflux for 2 h. The color of the solution changed gradually from red to violet. The solution was cooled to room temperature and the precipitated AgCl was separated by filtration through a sintered glass frit. An excess of $NaNO_2$ (103.5 mg, 1.5 mmol) was added to the filtrate and the mixture was heated under reflux for 6 h. After cooling to room temperature, the violet solution was reduced to 10 mL under vacuum and saturated aqueous NH_4PF_6 solution was added in excess. The precipitate thus obtained was filtered off, washed with water and Et_2O, and then dried in vacuo. Yield: 78.2 mg (77.4%) **^{1}H NMR** (400 MHz, CD_3OD) δ 9.25 (s, 2H), 9.11-9.04 (m, 2H), 8.69 (d, 2H), 8.00-7.96 (m, 2H), 7.50-7.44 (m, 3H), 7.25-7.21 (m, 2H), 6.05 (s, 2H), 2.49 (s, 6H), 1.93 (s, 6H) ppm. **ESI-MS** *m/z* $[M\text{-}PF_6^-]^+$: calcd 777.1, found 777.2.

Synthesis of [(tpy^{COOH})Ru(DAMBO)(NO)](PF_6)$_3$

Dropwise addition of 2.0 mL HNO_3 (2.0 mol·L^{-1}) directly to the solid [(tpy^{COOH})Ru(DAMBO)(NO_2)](PF_6) (100 mg, 0.11 mmol) at 273 K under stirring condition resulted in a pasty mass. A deep-red solid product was formed on addition of saturated aqueous NH_4PF_6 solution (5.0 mL). The precipitate was filtered off immediately, washed with cold water (2.0 mL) and Et_2O, and then dried in vacuo. Yield: 75.8 mg (58.4%). **^{1}H NMR** (400 MHz, CD_3OD) δ 9.24 (s, 2H), 9.04-8.93 (m, 2H), 8.74 (d, 2H), 8.15-8.08 (m, 2H), 7.51-7.48 (m, 2H), 7.13 (d, 1H), 7.02-6.97 (m, 2H), 6.07 (s, 2H), 2.52 (s, 6H), 1.81 (s, 6H) ppm. **ESI-MS** *m/z* $[M\text{-}3PF_6^-\text{-}2H^+]^+$: calcd 759.2, found 759.1. $[M\text{-}3PF_6^-\text{-}2H^+\text{-}NO]^+$: calcd 729.2, found 729.1. **FTIR** ν_{NO}: 1912 cm^{-1}.

Synthesis of {Ru-NO@TiO_2 NPs}.

In the typical process, 9.3 mg of (4-aminobenzyl) phosphonic acid (0.05 mmol) was dissolved in 2.0 mL of water at pH 9. Meanwhile, 10 mg of TiO_2 was sonicated in 18 mL of water. Subsequently, the (4-aminobenzyl)phosphonic acid solution was added to the stirred TiO_2 dispersion. The mixture was left stirring overnight under dark. The resulting dispersion was centrifuged at 10,000 rpm for 10 min and washed twice with water. The supernatant was decanted and the obtained NH_2@TiO_2 NPs were re-dispersed in water.

[(tpy^{COOH})Ru(DAMBO)(NO)]$(PF_6)_3$ (100 mg, 0.08 mmol) and FA (5.0 mg, 0.01mmol) were dissolved in 5.0 mL DMF, activated by an EDC/NHS solution for 30 min. Following that, 50.0 mg of NH_2@TiO_2 NPs was added to react for 12 h at room temperature. The excess reagents were removed as supernatant by centrifugation at 10,000 rpm for 10 min, and the precipitate was washed thrice with DMF and deionized water. Finally, the {Ru-NO@TiO_2 NPs} thus obtained were re-dispersed in water.

Light triggered NO release.

The {Ru-NO@TiO_2 NPs} nanoplatform (2.0 mg/mL) was suspended in saline solution (150 mM) in a quartz cuvette under gentle stirring using a magnetic stirring bar. Following that, NO release was initiated by irradiation of the sample cell with a 300 W Xenon lamp (Asahi Spectra Max 303 equipped with a 300–600 nm ultraviolet visible module, 1.0 collimator lens and a longpass filter UV400). The intensity of visible light irradiation (λ > 400nm) on the sample cell was measured by using a CEL-NP 2000 intensity meter. The amount of NO released was measured using a NO-sensitive electrode (World Precision Instrument, ISO-NO meter, equipped with a TBR1025 free radical analyzer for measuring nitric oxide from 0.3 nM to 100 μM.). The tip of the electrode was placed outside the light path. The electrode was accurately calibrated by mixing standard solutions of $NaNO_2$ with H_2SO_4 (0.1 M) and KI (0.1 M), according to the protocol indicated in the manufacturer manual. The amperometric data collected from the electrode was then converted into the corresponding nitric oxide concentration.

NO quantum yield measurement.

LED light source of BLR 470 nm, GRR 530 nm and RTR 627 nm were used for NO quantum yields measurement. Light intensity was determined before each photolysis experiments by an actinometry meter (measured intensity of ~ 5 mW). The solution of {Ru-NO@TiO_2 NPs} was placed in a 1.0 cm-path-length quartz cuvette, 1.0 cm away from the light source. The solution was prepared to ensure sufficient absorbance (>90 %) at the irradiation wavelength and agitated periodically under an argon atmosphere during the photolysis experiment. NO quantum yields (Φ_t) were calculated based on NO concentrations, obtained by NO meter measurement. The calculated values were plotted versus *t*. These plots were linear, with a negative slope, for the first 20-25% of the reaction. The extrapolated quantum yield at t = 0 (y intercept) was taken as Φ_{NO} for the photolabilization of NO from the {Ru-NO@TiO_2 NPs} solution.

Singlet oxygen ($^1O_2$) detection:

{Ru-NO@TiO_2 NPs}, {Ru-Cl@TiO_2 NPs} or TiO_2 NPs (80 mg) were added to a quartz reactor containing 100 mL of 1.6×10^{-4} M CHDDE aqueous solution. The solution was then irradiated by visible light while stirring (λ > 400nm, 300 mW/cm^2). Aliquots were withdrawn with 10 min intervals from each reactor. Collected samples were centrifuged, and the supernatant was analyzed by UV-vis spectroscopy. The concentration of CHDDE was determined from the absorbance at 270 nm.

Cell culture.

Human cervical carcinoma cells (HeLa cells) and human breast cancer cells (MCF-7 cells) were obtained from Shanghai Institutes for Biological Sciences (SIBS), Chinese Academy of Science (CAS, China). HeLa cells and MCF-7 Cells were cultured in Roswell Park Memorial Institute medium (RPMI-1640, Thermo, USA) and Dulbecco′s Modified Eagle Medium (DMEM, Thermo, USA) at 37 °C under 5% CO_2 atmosphere, supplemented with 10% (v/v) fetal bovine serum (Gibco, USA) and 1% (v/v) penicillin/streptomycin.

MTT assay.

All the cells were seeded on a 96-well plate with a density of 5×10^4 cells per well and incubated in a humidified 5% CO_2 atmosphere for 24 h. The cell culture medium were removed and washed

with PBS. Following that, different concentrations of the {Ru-NO@TiO_2 NPs} nanoplatform (0, 50, 100, 200, 400 μg/mL) suspended in cell culture medium were added and incubated further for a period of 12 or 24 h at 37 °C in a humidified 5% CO_2 atmosphere. MTT (20 μL, 5.0 mg/mL) solution was added to each well. After 4 h of incubation at 37 °C, the cell culture medium was removed and the formazan crystals were lysed with 150 μL of DMSO. The absorbance was then measured at 490 nm using a microplate reader (Multiskan MK3, USA).

Visible light irradiation experiments: After incubation of the cells with different concentrations of the {Ru-NO@TiO_2 NPs} nanoplatform (0, 50, 100, 200, 400 μg/mL) for 4 h, light irradiation was applied (λ > 400nm, 200 mW/cm^2, 10 min), and the cells were incubated for another 6 or 12 h. Subsequently, the same procedures, as described above, were performed to obtain the final absorbance measurement at 490 nm using a microplate reader.

Confocal laser scanning microscopy.

Fluorescence imaging was performed with a Leica DMI 6000B confocal scanning system. A 405 nm laser was used as the excitation source and the corresponding emissions were collected in the wavelength range of 425–475 nm. HeLa and MCF-7 cells were seeded on a plastic-bottomed μ-dish of diameter 35 mm, with a density of 10^4 cells and maintained at 37 °C in 5% CO_2 atmosphere for 24 h. The cells were then treated with the {Ru-NO@TiO_2 NPs} solution (50 μg/mL) for 2h. After incubation, the cells were washed twice with PBS and subjected to confocal fluorescence microscopy analysis.

Real-time intracellular NO detection experiments: After incubating the cells with the {Ru-NO@TiO_2 NPs} solution (50 μg/mL) in the cell culture medium for 8 h, the cells were washed twice with PBS, treated with DAF-FM-DA (5 μM), and then incubated for 30 min. After the incubation period, the cells were washed twice with PBS and imaged with serum-free medium in the absence or presence of light irradiation (λ > 400nm, 200 mW/cm^2, 1 min). Excitation was carried out with lasers at λ = 405 nm or 488 nm, and emissions were recorded in the wavelength range of 425–475 nm or 500–550 nm, respectively.

Intracellular $^1O_2$ detection experiments: After incubating the cells with the {Ru-NO@TiO_2 NPs} solution (100 μg/mL) in the cell culture medium for 3 h, the cells were washed twice with PBS, treated with DCFH-DA (5 μM) and then incubated for 20 min. After the incubation period,

the cells were washed twice with PBS and imaged with serum-free medium in the absence or presence of light irradiation (λ > 400nm, 300 mW/cm^2, 100 s). Excitation was carried out with lasers at λ= 405 nm and 488nm, and emissions were collected in the wavelength range of 425–475nm or 500–550 nm, respectively.

Flow Cytometry (FCM).

For receptor-directing binding experiments, HeLa and MCF-7 cells were incubated with {Ru-NO@TiO_2 NPs} solution (50 μg/mL) in cell culture medium for 2 h at 37 °C. Similarly, for the competitive binding experiments, HeLa cells were pre-incubated with free folic acid (50 μg/mL) for 30 min and then further incubated with the {Ru-NO@TiO_2 NPs} solution (50 μg/mL) for 2 h at 37 °C. All the cells were washed twice with PBS and harvested by trypsinization, followed by centrifugation at 1,500 rpm for 6 min. The precipitate thus obtained was re-suspended in PBS and analyzed using a flow cytometer.

For intracellular $^1O_2$ detection experiments: HeLa cells were incubated with {Ru-NO@TiO_2 NPs}, {Ru-Cl@TiO_2 NPs} and TiO_2 NPs solution (100 μg/mL) in cell culture medium for 3 h at 37 °C, respectively. The cells were washed twice with PBS, treated with DCFH-DA (10 μM) and then incubated for 20 min. After visible light (λ > 400 nm, 300 mW/cm^2, 100 s) irradiation, the cells were washed twice by PBS and detached by trypinization, followed by centrifugation at 1,500 rpm for 6 minutes. The precipitate thus obtained was re-suspended in PBS and analyzed using a flow cytometer.

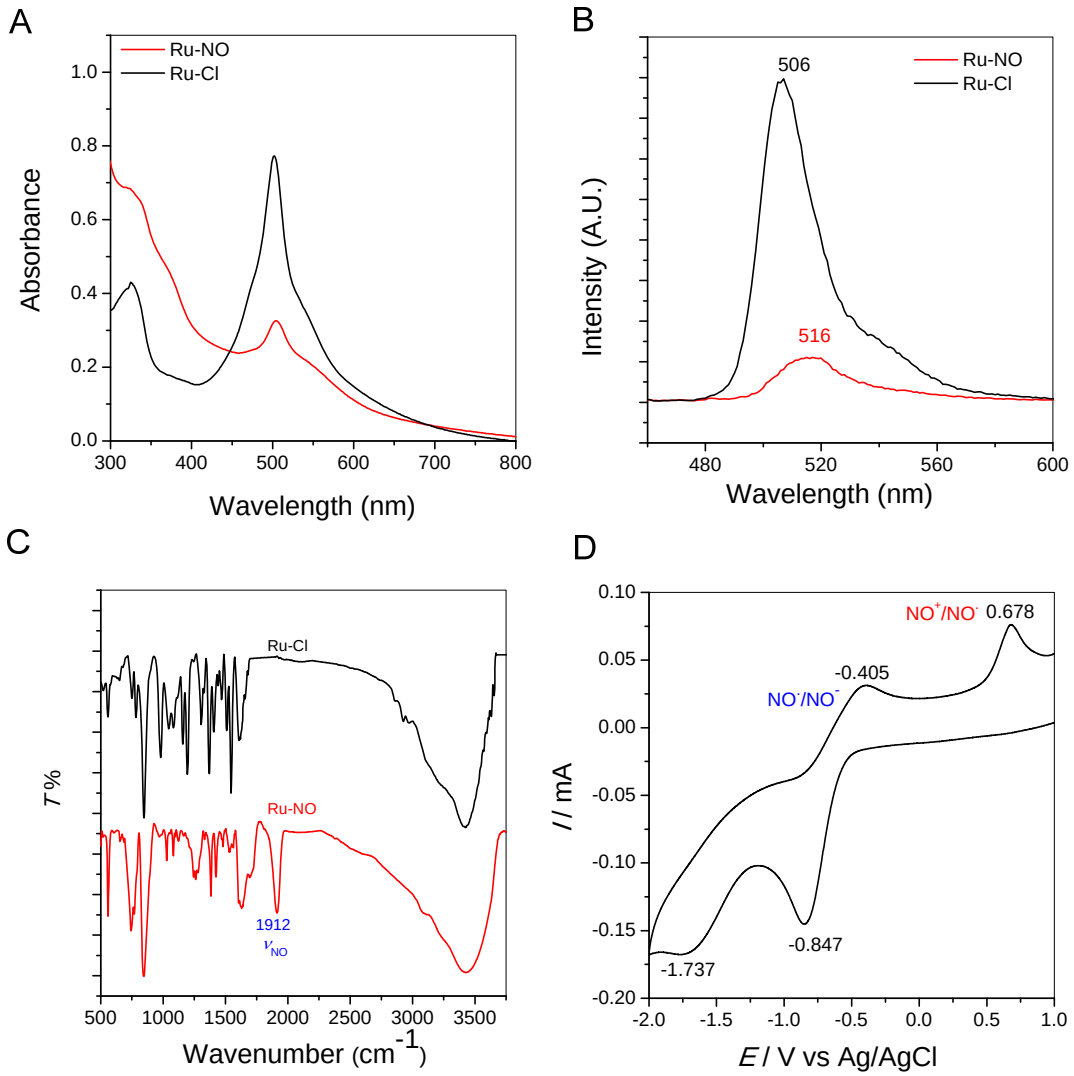

Figure S1 Spectroscopic characterization of [(tpy^{COOH})Ru(DAMBO)(NO)](PF$_6$)$_3$ (A) UV-vis spectra of [(tpy^{COOH})Ru(DAMBO)(NO)]$^{3+}$ (red), and [(tpy^{COOH})Ru(DAMBO)(Cl)]$^{+}$ (black) in DMF solution. (B) Fluorescence spectra of [(tpy^{COOH})Ru(DAMBO)(NO)]$^{3+}$ (red) and [(tpy^{COOH})Ru(DAMBO)(Cl)]$^{+}$ (black) in CH_3CN. Ex.: 450 nm. (C) FT-IR spectra of [(tpy^{COOH})Ru(DAMBO)(NO)]$^{3+}$ (red), and [(tpy^{COOH})Ru(DAMBO)(Cl)]$^{+}$ (black). (D) Cyclic voltammogram of [(tpy^{COOH})Ru(DAMBO)(NO)]$^{3+}$ in CH_3CN with 0.1 M *n*-Bu_4NBF_4 as the electrolyte. Scan rate: 100 mV/s.

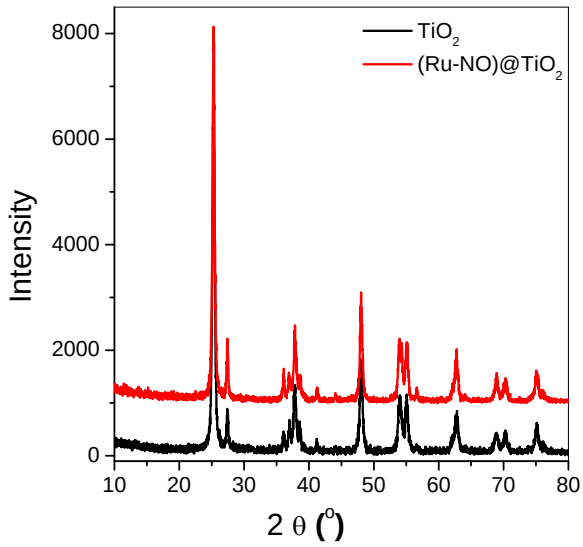

Figure S2 XRD patterns of the {Ru-NO@TiO_2 NPs} nanoplatform (red), and unmodified TiO_2 (black).

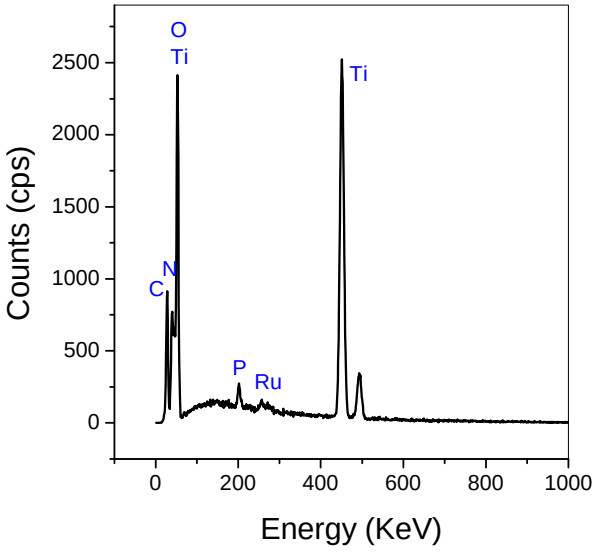

Figure S3 EDS spectrum of the {Ru-NO@TiO_2 NPs} nanoplatform.

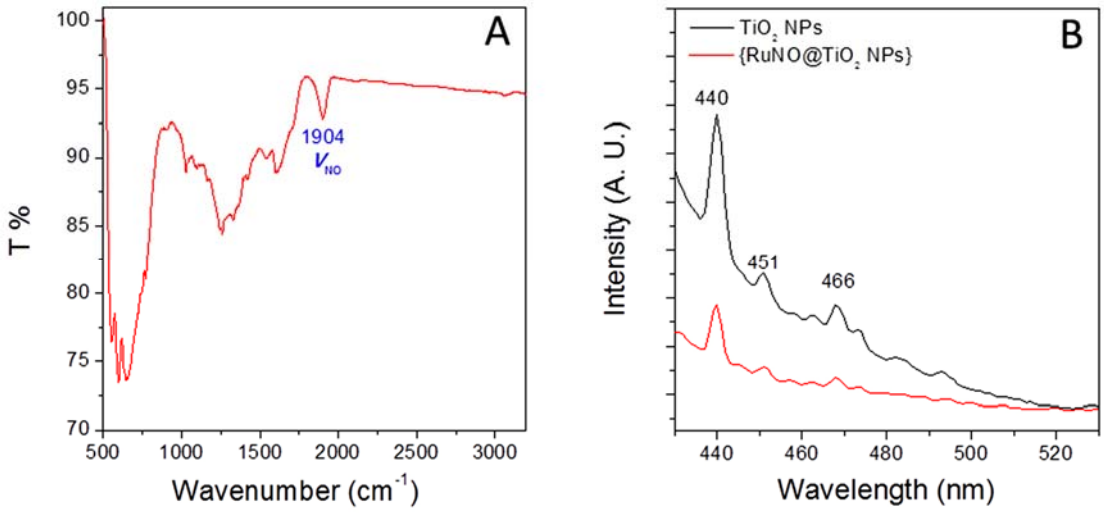

Figure S4 (A) FT-IR spectra of the {Ru-NO@TiO_2 NPs} nanoplatform. (B) Photoluminescence spectra of the {Ru-NO@TiO_2 NPs} nanoplatform (red line) and TiO_2 NPs (black line). Ex: 400 nm

In semiconductor such as TiO_2-based material, the PL spectra are related to the transfer behavior of the photoinduced electrons and holes, reflecting the separation and recombination of photoinduced charge carriers. The PL spectra have thus been widely used to examine the efficiency of charge carrier trapping, migration and transfer to understand the fate of electron-hole pairs (H. Fu, *et al. J. Phys. Chem. B*, 2005, *109*, 2805; J. Zhang, *et al. Chem. Eng. J.* 2014, *236*, 388; G. Fu, *et al. J. Phys. Chem. B*, 2006, *110*, 17860; S. B. Ogale, *et al. J. Phys. Chem. C*, 2008, *112*, 14595.). The multiple peaks observed at 440, 451, and 466 nm reflected different band gap transition or charge carrier transitions in the TiO_2-based nanoplatform. The surface modification by ruthenium nitrosyl reduced the intensity of the PL spectra relative to that of the unmodified TiO_2, which suggests enhanced contribution of non-irradiation process and the recombination of electron and holes was declined. This phenomenon is consistent with the photoinduced electron transfer to the Ru-NO site whereby promoting NO-release.

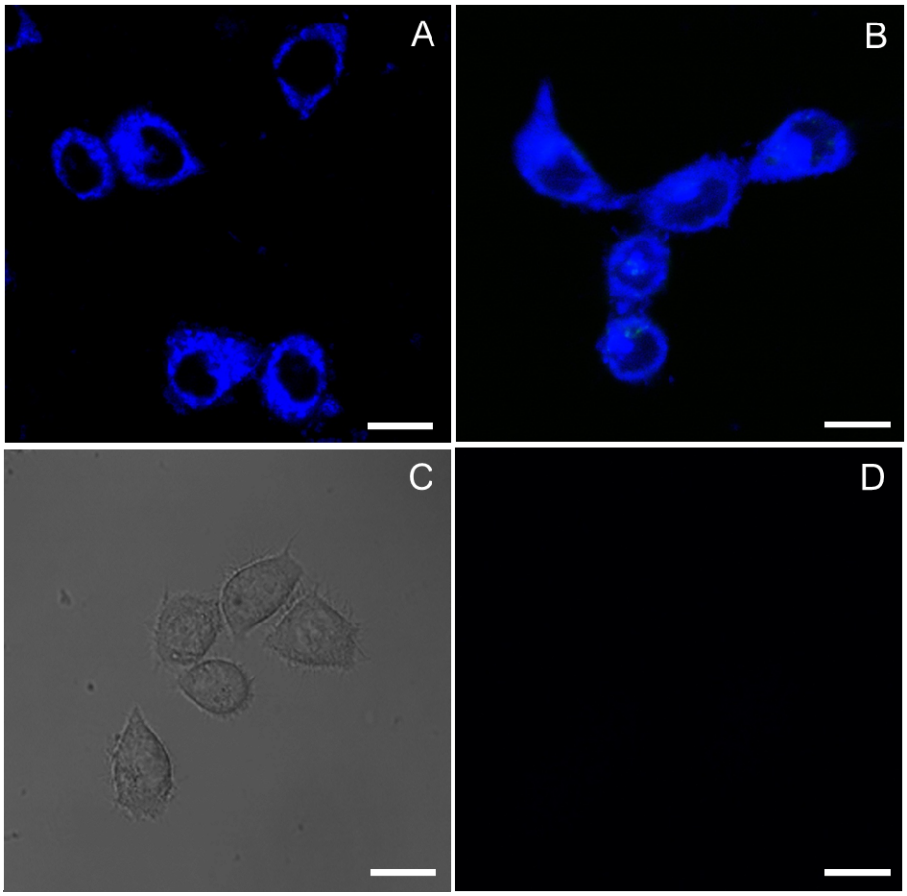

Figure S5 Confocal microscopy images of FR (+) HeLa cells treated with 50 μg/mL of the nanoplatform for 30 min (A), and 8h (B) at 37 °C, respectively. Control: confocal microscopy images of FR (+) HeLa cells in the absence of the nanoplatform (C: bright field; D: dark field). The samples were excited at the wavelength of 405 nm and the corresponding fluorescence was recorded in the range of 425–475 nm. Scale bar: 15 μm.

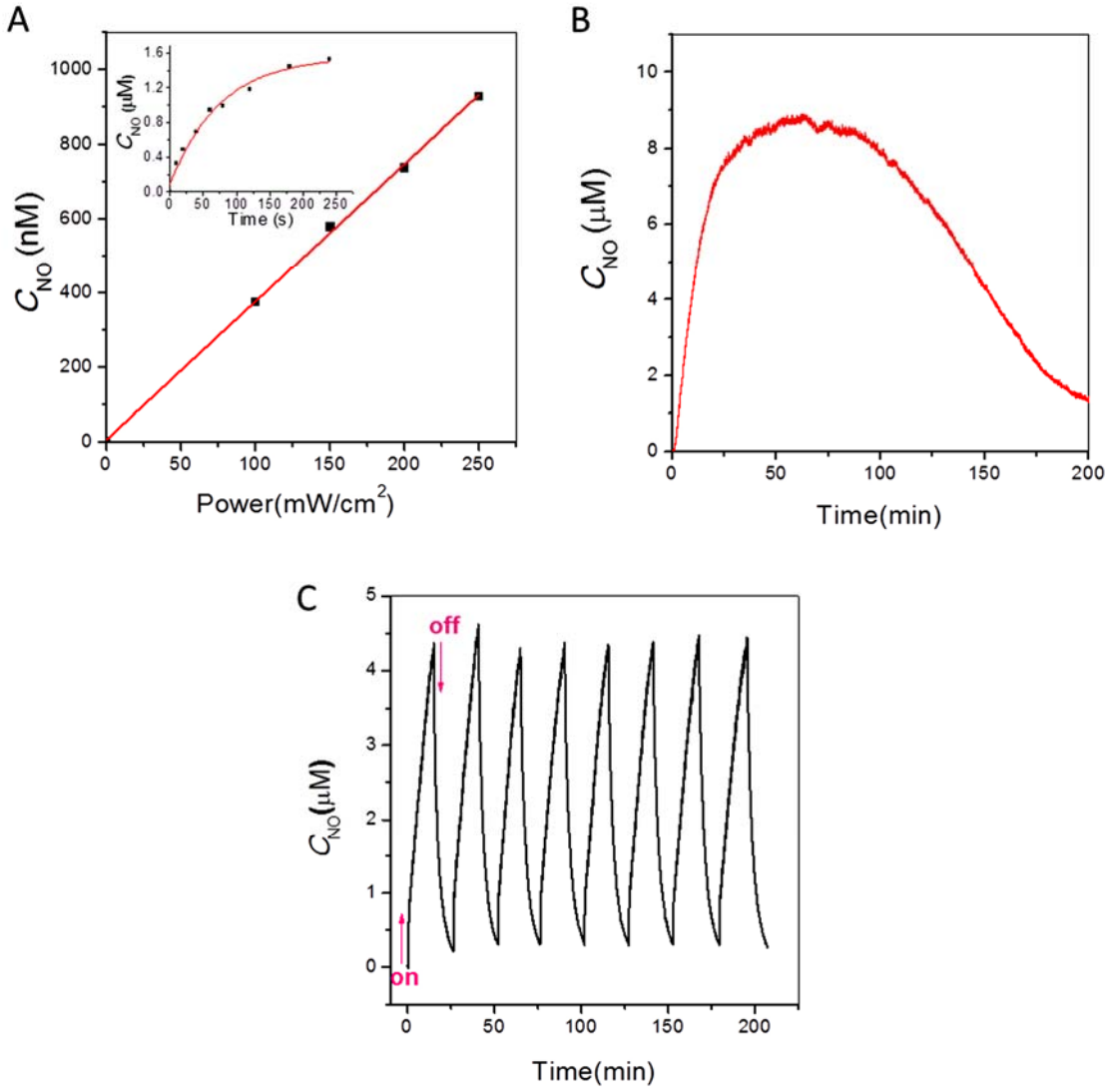

Figure S6 (A) Correlation of the amount of NO release from 2.0 mg/mL {Ru-NO@TiO_2 NPs} suspended in saline solution with the applied light intensity (30 s of duration time). Inset shows the correlation of released NO with the duration of light. (B) Light-induced NO release from 1.0 mg/mL {Ru-NO@TiO_2 NPs} suspended in aerobic saline solution by constant light illumination (λ > 400 nm, 300 mW/cm^2). (C) NO flux from 2.0 mg/mL {Ru-NO@TiO_2 NPs} suspended in aerobic saline solution triggered by periodic light illumination (300 mW/cm^2, 15 min). Light source: xenon lamp of wavelength λ > 400 nm with longpass filter.

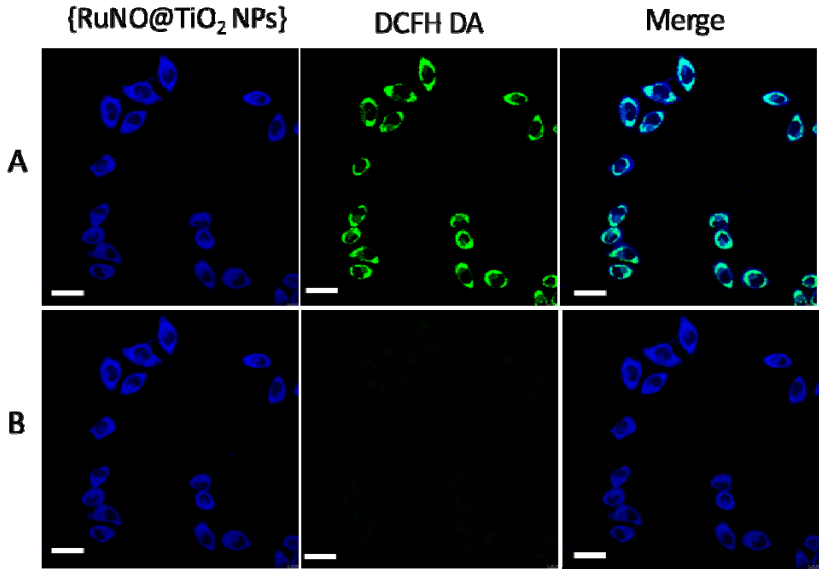

Figure S7 Subcellular localization of ROS generated during {Ru-NO@TiO_2 NPs}-mediated PDT by DCFH-DA. (A) Confocal microscopy images of HeLa cells treated with the nanoplatform (50 μg/mL) and DCFH-DA (5 μM) after visible light irradiation (> 400 nm, 300 mW/cm^{-2}, 100 s). (B) Control cells without irradiation. The blue and green images were obtained for excitation at 405 and 488 nm, and recording the corresponding fluorescence in the range of 425–475, and 500–550 nm, respectively. Scale bar: 30 μm.

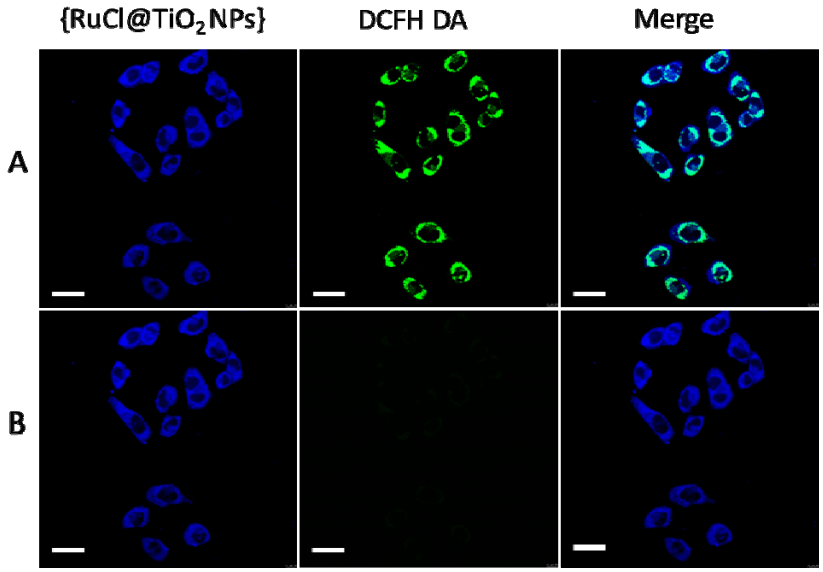

Figure S8 Subcellular localization of ROS generated during {Ru-Cl@TiO_2 NPs}-mediated PDT by DCFH-DA. (A) Confocal microscopy images of HeLa cells treated with the nanoplatform (50 μg/mL) and DCFH-DA (5 μM) after visible light irradiation (> 400 nm, 300 mW/cm^{-2}, 100 s). (B) Control cells without irradiation. The blue and green images were obtained for excitation at 405 and 488 nm, and recording the corresponding fluorescence in the range of 425–475, and 500–550 nm, respectively. Scale bar: 30 μm.

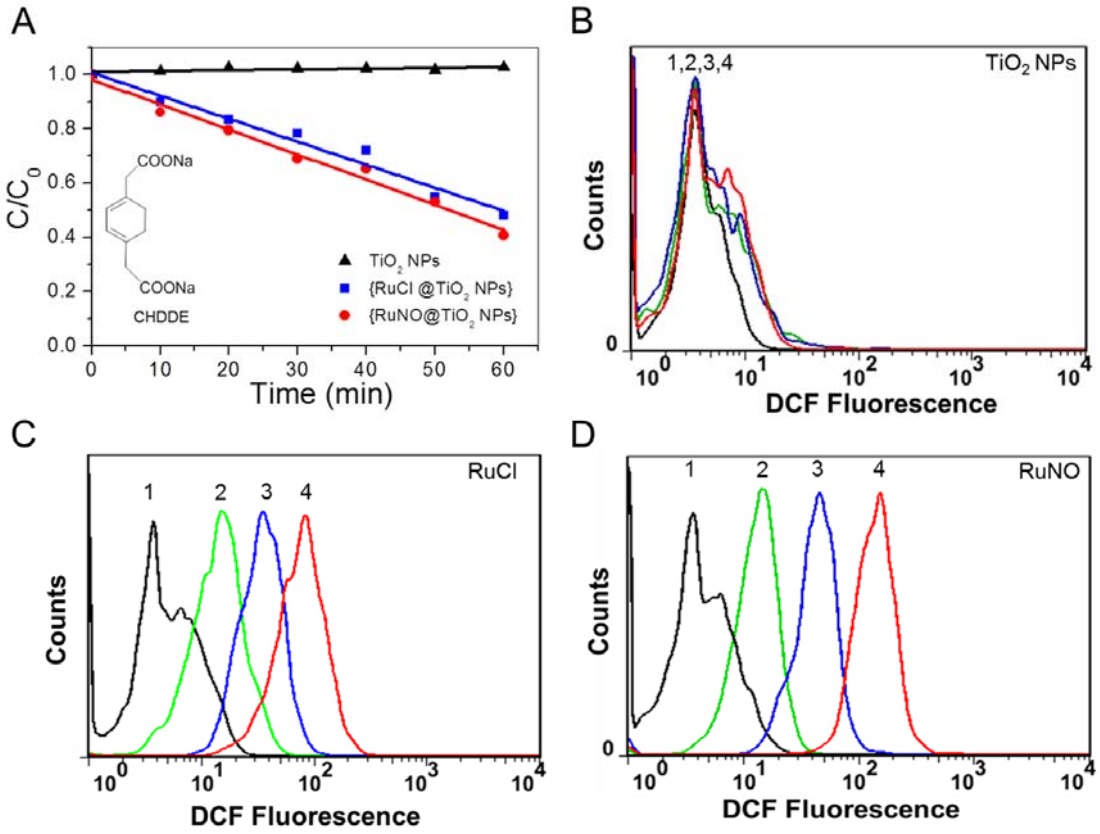

Figure S9 (A) Singlet oxygen species detection by a $^1O_2$ trap CHDDE. Plot of CHDDE relative concentration versus irradiation time catalyzed by {Ru-NO@TiO_2 NPs} (filled circle), {Ru-Cl@TiO_2 NPs} (filled square), and TiO_2 NPs (filled triangle), respectively. Light source: xenon lamp of wavelength $\lambda > 400$ nm with longpass filter (300 mW/cm^2). **(B)** Flow cytometric detection of ROS with a probe of DCFH-DA. FR (+) HeLa cells were treated with the {TiO_2 NPs} nanoplatform (200 μg/mL), DCFH-DA (10 μM), and followed by visible light irradiation (> 400 nm, 300 mW/cm^2) on different exposure time (**1**: 0; **2**: 100 s; **3**: 300 s; **4**: 500 s). **(C)** Flow cytometric detection of ROS with a probe of DCFH-DA. FR (+) HeLa cells were treated with the {RuCl@TiO_2 NPs} nanoplatform (200 μg/mL) DCFH-DA (10 μM), and followed by visible light irradiation (> 400 nm, 300 mW/cm^2) on different exposure time (**1**: 0; **2**: 100 s; **3**: 300 s; **4**: 500 s). **(D)** Flow cytometric detection of ROS with a probe of DCFH-DA. FR (+) HeLa cells were treated with the {RuNO@TiO_2 NPs} nanoplatform (200 μg/mL), DCFH-DA (10 μM), and followed by visible light irradiation (> 400 nm, 300 mW/cm^2) on different exposure time (**1**: 0; **2**: 100 s; **3**: 300 s; **4**: 500 s).

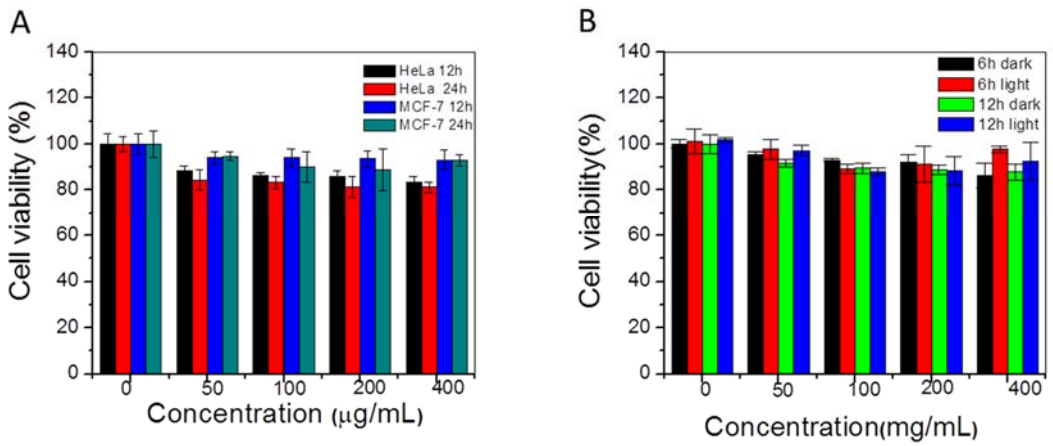

Figure S10 (A) Dark lethality of FR (+) HeLa and FR (-) MCF-7 cells treated with the {Ru-NO@TiO_2 NPs} nanoplatform of concentration ranging from 0 to 400 μg/mL for the incubation time of 12 h and 24 h, respectively. (B) Dark and photo-induced lethality of HeLa cells treated with the {FA@TiO_2 NPs} nanoplatform of concentration ranging from 0 to 400 μg/mL for the incubation time of 6 h and 12 h, respectively. Irradiation with visible light (> 400 nm, 200 mW/cm^{-2}, 10 min).

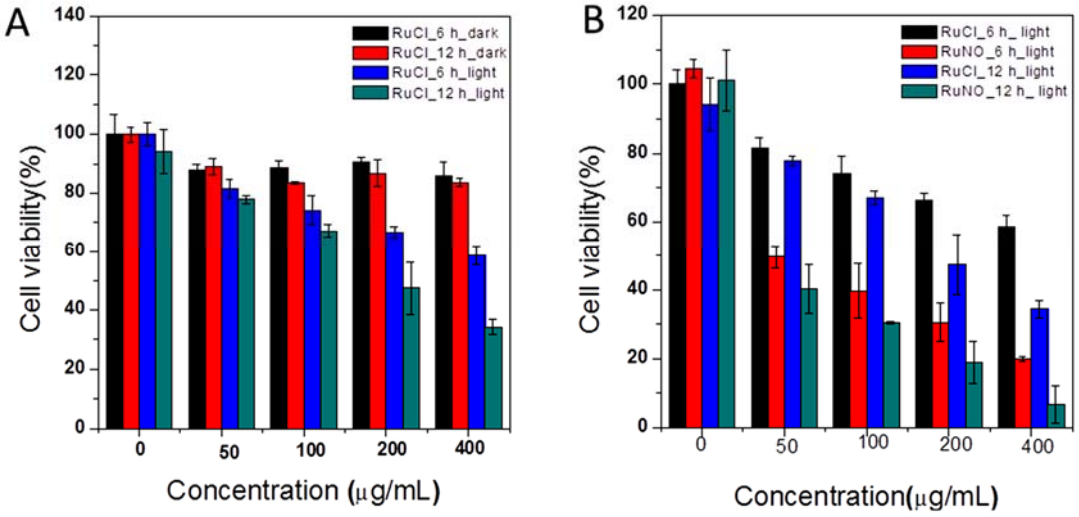

Figure S11 (A) Dark and photo-induced lethality of HeLa cells treated with the {Ru-Cl@TiO_2 NPs} nanoplatform of concentration ranging from 0 to 400 μg/mL for the incubation time of 6 h and 12 h, respectively. Irradiation with visible light (> 400 nm, 200 mW/cm^{-2}, 10 min). (B) Mortality of HeLa cells treated with {Ru-NO@TiO_2 NPs} and {Ru-Cl@TiO_2 NPs} at different concentrations (0 to 400 μg/mL) under visible light illumination (> 400 nm, 200 mW/cm^{-2}, 10 min), followed by incubation for 6 h and 12 h at 37 °C, respectively.

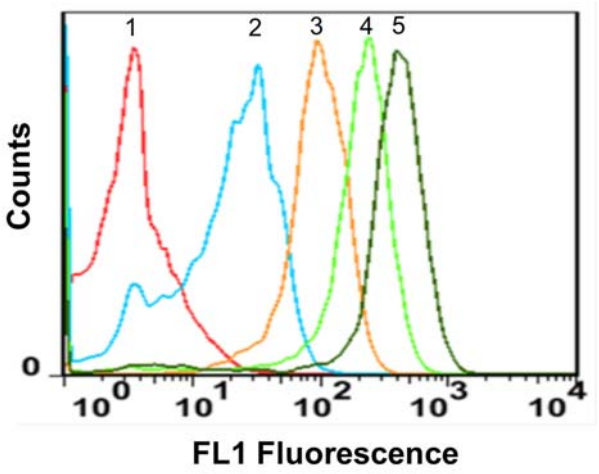

Figure S12 Flow cytometric analysis of FR (+) HeLa cells treated with different concentrations of the {Ru-NO@TiO_2 NPs} nanoplatform (1: 0; 2: 50; 3: 100; 4: 200; 5: 400 μg/mL) under visible light irradiation (> 400 nm, 200 mW/cm^2, 10 min).

The intensity of apoptosis fluorescence was found to increase significantly with increase in the concentration of the nanoplatform. The increasing trend was in accordance with the results observed in cytotoxicity studies.

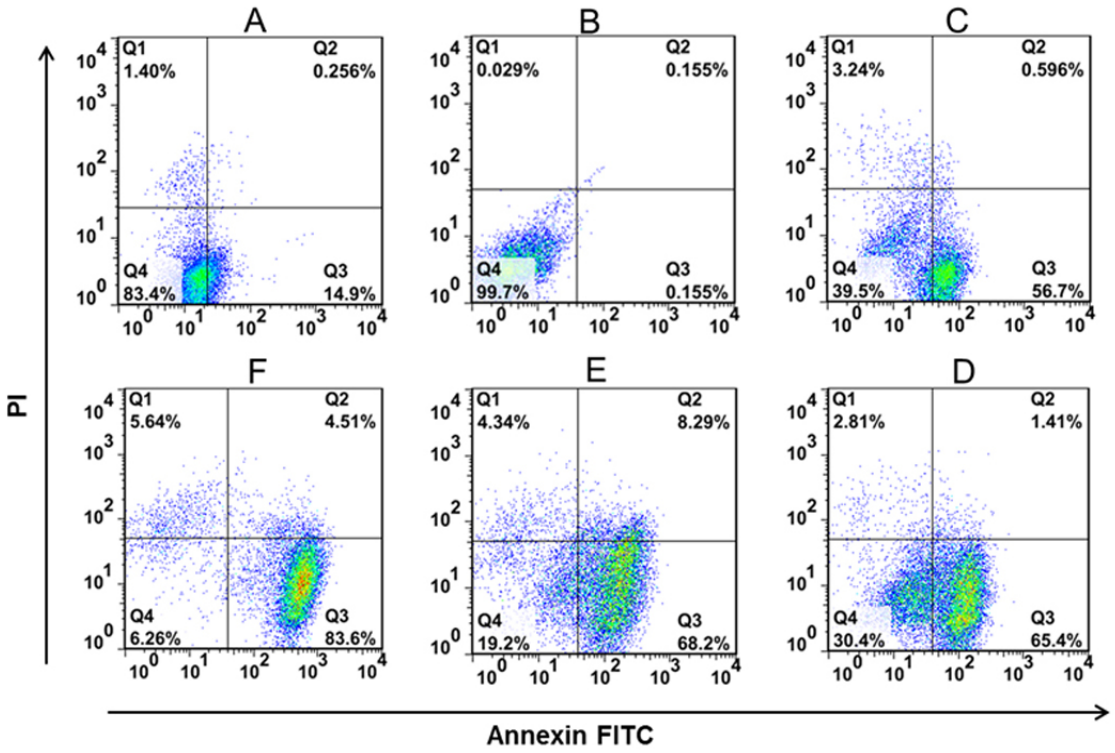

Figure S13 Flow cytometric analysis for early and late apoptotic cells. (A) Control: HeLa cells were treated with 400 μg/mL of the {Ru-NO@TiO_2 NPs} nanoplatform under dark and incubated for 12 h. (B) Control: HeLa cells were irradiated by visible light (> 400 nm, 200 mW/cm^{-2}, 10 min) in the absence of the nanoplatform and incubated for 12 h. From (C—F): HeLa cells were treated with the {Ru-NO@TiO_2 NPs} nanoplatform in the concentration of 50 (C), 100 (D), 200 (E), and 400 (F) μg/mL, irradiated by visible light (> 400 nm, 200 mW/cm^{-2}, 10 min), and then followed by incubation of 12 h, respectively.

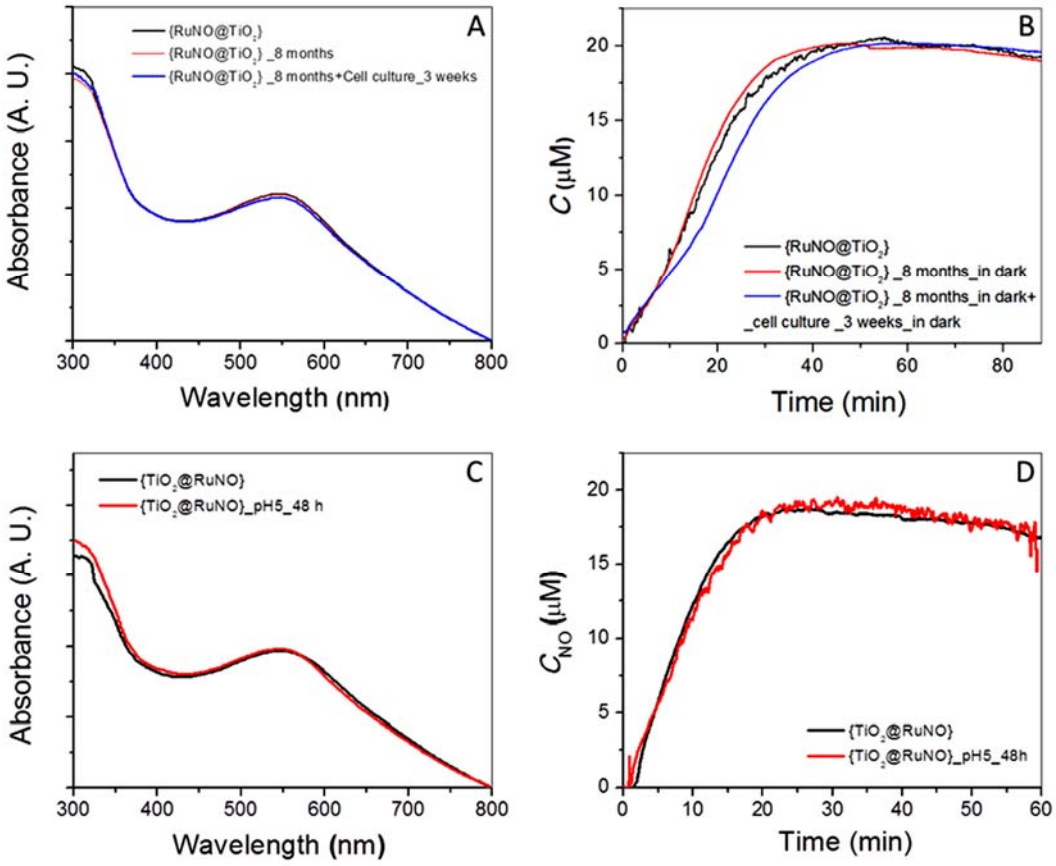

Figure S14 Stability test of the {Ru-NO@TiO_2 NPs} nanoplatform . (A) Diffuse reflectance UV-vis spectra of the {Ru-NO@TiO_2 NPs} nanoplatform. Black line: nanoplatform tested initially; red line: after 8 months-storage in the dark as solid; blue line: 8 months-storage in the dark as solid and further keeping in cell culture for 3 weeks in the dark. Cell culture was composed of RPMI 1640 medium/fetal bovine serum (V:V = 9:1). (B) Light-induced NO release from 2.0 mg/mL {Ru-NO@TiO_2 NPs} suspended in saline solution by constant light illumination (300 mW/cm^2). Black line: nanoplatform tested initially; red line: after 8 months-storage in the dark as solid; blue line: 8 months-storage in the dark as solid and further keeping in cell culture for 3 weeks in the dark. Cell culture was composed of RPMI 1640 medium/fetal bovine serum (V:V = 9:1). (C) Diffuse reflectance UV-vis spectra of the {Ru-NO@TiO_2 NPs} nanoplatform. Black line: nanoplatform tested initially in acidic saline solution (pH = 5.0); red line: after 48 h storage in acidic saline solution (pH = 5.0) in the dark. (D) Light-induced NO release from 2.0 mg/mL {Ru-NO@TiO_2 NPs} suspended in acidic saline solution (pH = 5.0) by constant light illumination (300 mW/cm^2). Black line: nanoplatform tested initially; red line: after 48 h storage in acidic saline solution (pH = 5.0) in the dark.

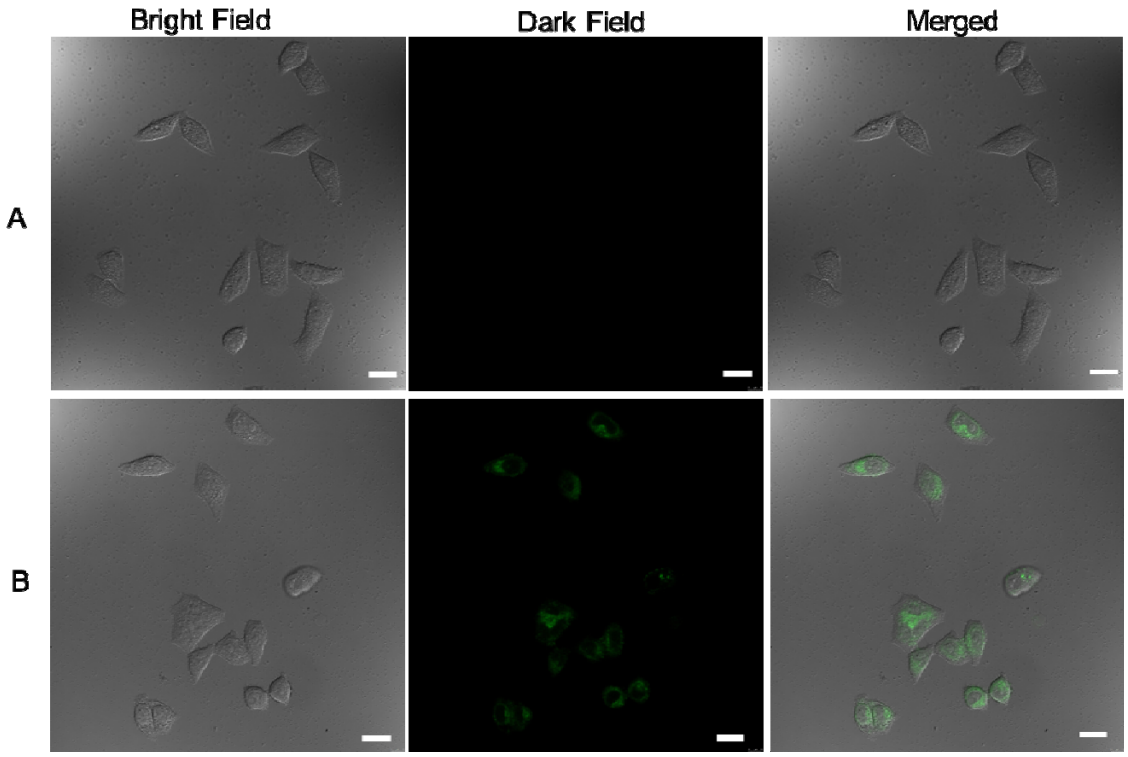

Figure S15 3 Confocal microscopy images of HeLa cells treated with $[Ru^{II}(tpy^{COOH})(DAMBO)NO](PF_6)_3$, (**1**), solution (42 μM in 3% DMSO/H_2O) for 30 min (A) and 3 h (B) at 37 °C, respectively. The samples were excited at the wavelength of 488 nm and the corresponding fluorescence was recorded in the range of 500–550 nm. Scale bar: 20 μm. For the sample with 30 min incubation, there was no fluorescence observed, and after 3h incubation, very weak green fluorescence was noticed.

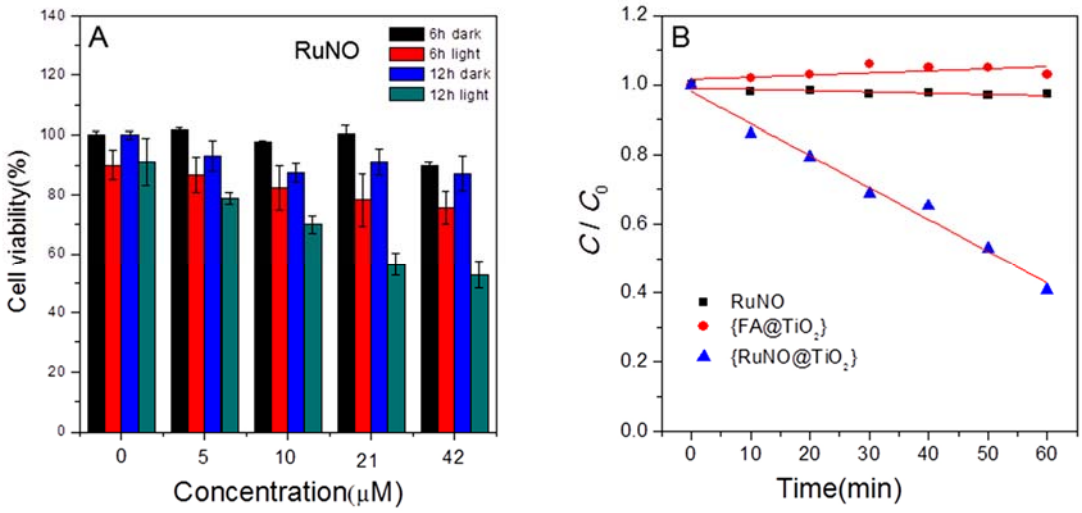

Figure S16 (A) Dark and visible light-induced (10 min.) lethality of HeLa cells treated with different concentration of $[Ru^{II}(tpy^{COOH})(DAMBO)NO](PF_6)_3$ (**1**, Ru-NO) (0 ~ 42 μM in 3% DMSO/H_2O solution) for incubation of 6 h and 12 h, respectively. The amount of ruthenium nitrosyl in **1** with concentration of 0 ~ 42 μM approximately corresponds to those in the {RuNO@TiO_2} nanoplatform with concentration of 0 ~ 400 μg/mL. (B) Singlet oxygen species detection by a $^1O_2$ trap CHDDE. Plot of CHDDE relative concentration versus irradiation time catalyzed by {Ru-NO@TiO_2 NPs} (filled triangle), {FA@TiO_2 NPs} (filled circle), and **1** (filled square, **1** was dissolved in 4% DMF/H_2O), respectively. Light source: xenon lamp of wavelength λ > 400 nm with longpass filter (300 mW/cm^2).

References:

S1. Gabe, Y.; Urano, Y.; Kikuchi, K.; Kojima, H.; Nagano, T. *J. Am. Chem. Soc.* **2004**, *126*, 3357-3367.

S2. Choong, C.; Foord, J. S.; Griffiths, J.-P.; Parker, E. M.; Luo, B.; Bora, M.; Moloney, M. G. *New J. Chem.* **2012**, *36*, 1187.

S3. Constable, E. C.; Dunphy, E. L.; Housecroft, C. E.; Neuburger, M.; Schaffner, S.; Schaper, F.; Batten, S. R. *Dalton Trans.* **2007**, 4323.

S4. Park, H.-J.; Kim, K. H.; Choi, S. Y.; Kim, H.-M.; Lee, W. I.; Kang, Y. K.; Chung, Y. K. *Inorg. Chem.* **2010**, *49*, 7340-7352.

S5. Nardello, V.; Azaroual, N.; Cervoise, I.; Vermeersch, G.; Aubry, J. M. *Tetrahedron* **1996**, *52*, 2031-2046.